UCRL-ID-135122

Energetics of Crystalline Silicon Dioxide-Silicon (SiO_2/Si) Interfaces

Thomas J. Lenosky
Andrew Chizmeshya
Otto F. Sankey
Alexander A. Demkov

7/14/99

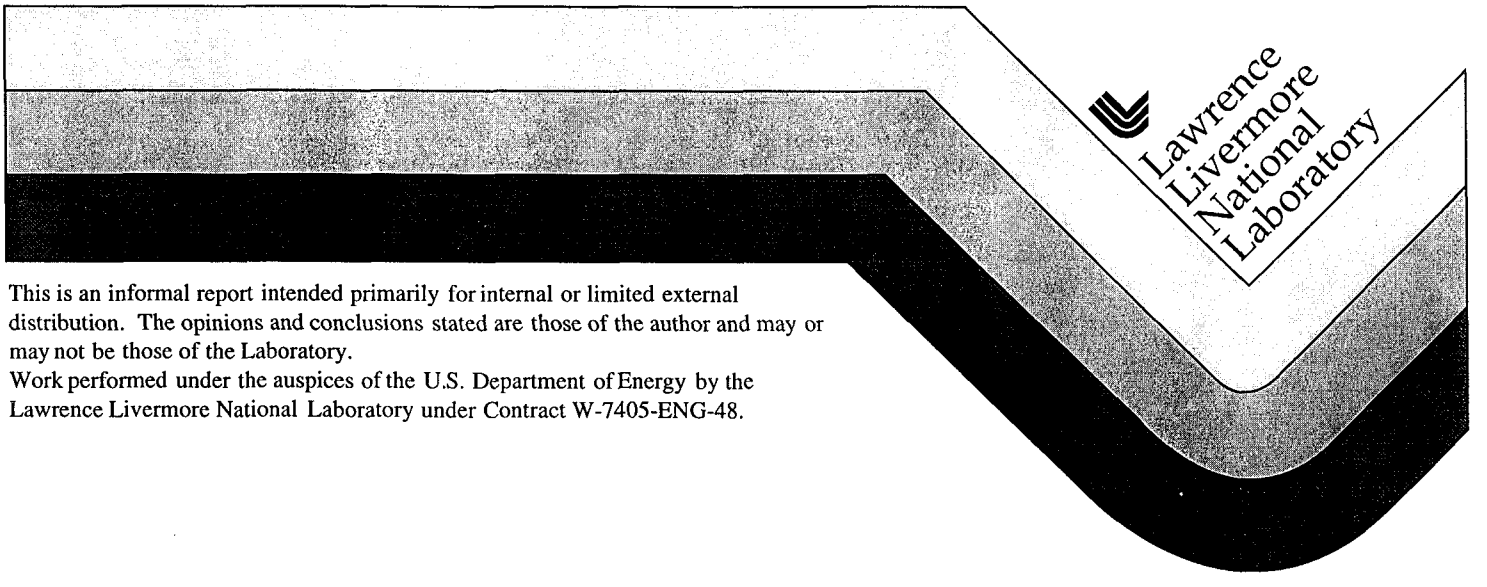

Work performed under the auspices of the U.S. Department of Energy by the Lawrence Livermore National Laboratory under Contract W-7405-ENG-48.

Energetics of Crystalline Silicon Dioxide–Silicon (SiO_2/Si) Interfaces

Thomas J. Lenosky, Andrew Chizmeshya, and Otto F. Sankey

Department of Physics and Astronomy, Arizona State University, Tempe, Arizona 85287-1504

Alexander A. Demkov

Predictive Engineering Laboratory, Motorola, Inc., Mesa AZ 85202

(September 10, 1998)

Abstract

We consider the interface between a (100) silicon surface and several naturally occuring crystalline silicon dioxide (SiO_2–silica) polymorphs: α–quartz, β–cristobalite, tridymite, and keatite. Using a classical empirical potential, we compute the strain energy required for epitaxy for each silica structure. Tridymite is the least energetically favorable epitaxial phase, followed by α–quartz, then β–cristobalite, while the most energetically favorable phase is keatite. We discuss the implications of this for epitaxial growth, and the crystalline to amorphous transition within atomically thin silica layers.

Silicon dioxide (silica, or SiO_2) is used in modern integrated circuits as an insulating layer. In a metal–oxide semiconductor field–effect transistor (MOSFET), silica forms the insulating layer between the metal gate and the silicon conduction channel. For this and other reasons, it is important to understand the structure of SiO_2 thin films and their electrical properties. Generally, silica forms almost atomically flat interfaces which introduce very few electronic states within the silicon gap. The (100) surface of silicon is the most important surface for integrated circuit manufacture, so we will limit our study to this surface.

Silica formed by oxidizing a silicon surface is generally thought to be amorphous, except

perhaps for a thin crystalline layer of SiO_2 between the silicon substrate and the amorphous layer. It is this thin crystalline layer which is the topic of the present work. The existance of this thin crystalline layer is still controversial, and an aim of the present work is to examine possible morphologies of the crystalline layers and their enbergetics to theoretically determine the plausibility of their existance. We have studied theoretically interfaces with four crystalline silica polymorphs: α–quartz, β–cristobalite, keatite, and tridymite[1]. Because the lattice constants of all the phase considered differ significantly from those of silicon, epitaxial growth of these phases would result in considerable strain. Presumably it is this strain energy that drives the oxide toward an amorphous state. In this work, we have evaluated this strain energy using a classical force field developed by van Beest *et al.*[2], which is a revised version of the model of Tsuneyuki *et al.*[3] These empirical potentials have been shown to describe the elastic properties of silica polymorphs with reasonable accuracy[2], and their shortcomings have been studied[4,5].

Experimentally, there is X–ray diffraction evidence for cristobalite crystallites[6–9] within the silica layer. Both compressed and elongated lattice constants for the cristobalite have been identified. There also is evidence for a thin tridymite layer at the interface[10], from electron diffraction, although this proposition has been questioned[11,12]. Most recently, Herbots et al. have found evidence of ordering in thin SiO_2 films on Si (100) using ion channeling combined with nuclear resonance analysis[13]. One possible reason for the variation in experimental results is that the preparation method of the silica interface appears to play an important role.

In the present work, we will investigate only the strain energy contribution to the growth of the interface, and neglect the energy due to the detailed local bonding immediately at the interface. Thus we evaluate how the energy of the interface increases as the silica layer grows thicker. This energy increase drives the system amorphous and causes it to form defects. Questions concerning the initial stages of the growth are not considered, as well as the energetics of passivation of dangling bonds. These questions are best answered by electronic structure methods. Of course, the unfavorable bond lengths and chemical bonds

formed at the interface may be energetically costly, and block the growth of even a low strain polymorph. Electronic structure methods to treat the initial phases and thicker layers are just becoming possible[14,15].

The β–cristobalite/Si interface is the simplest to visualize and has been studied theoretically by others. Hattori *et al.*[16] consider β–cristobalite with a compressed lattice constant, matched to Si (100). The a axis of β–cristobalite was compressed from 4.93 Å (experimental) to 3.83 Å. In the present work, we chose to consider only the expanded case, where the a axis is stretched to 5.43 Å. In this configuration, half of the silicon bonds at the interface are left dangling. Herman and Kasowski[17], and Hane *et al.*[18] left these bonds dangling, while Kageshima *et al.*[19] added oxygen at the interface to terminate them with Si–O double bonds. A third possibility exists: simply replacing each silicon interface atom that has two dangling bonds with an oxygen. A β–cristobalite interface with dangling bonds at the interface is shown in Fig. 1.

The tridymite interface structure proposed by Ourmazd *et al.*[10] also has dangling bonds at the interface. These can be removed either by direct dimerization, or by adding bridging oxygen atoms (as proposed by Ourmazd *et al.*). A recent theoretical study treated this tridymite interface[20]. The atomic structure of an undimerized tridymite interface is shown in Figs. 2a and 2b, for two different projections.

The interface between α–quartz and silicon has not been considered by previous authors. We find that the epitaxial strain and corresponding energy (see below) for this interface are not large, as one might first expect. There is ambiguity in terminating or rebonding dangling bonds at the interface as in the other polymorphs, and we propose an interface whose atomic structure is shown in Fig. 3. Notably, some of the oxygen atoms at the interface have three silicon neighbors, which may introduce strain at the interface.

The interface between keatite and silicon is also novel, and here we find the epitaxial strain and corresponding energy are the least among the polymorphs studied. For our proposed interfacial structure, one in four of the silicon atoms at the interface has two dangling bonds. A possible structure is shown in Fig. 4.

Silica polymorphs must be strained in order to be epitaxially bonded to the (100) silicon surface. We now estimate the energy cost of this epitaxial strain using the van Beest *et al.*[2] model. The silicon lattice parameter (5.43 Å) was assumed to be fixed. We estimated strain energy by examining single unit cells of the bulk silica structure in distorted geometries. We forced the cell dimensions to be commensurate with the Si lattice parameter in one plane, and allow the bulk silica to freely relax internally and normal to the surface. Periodic boundary conditions were used in all three directions.

The van Beest *et al.* model has three terms:

$$\Phi_{ij} = q_i q_j / r_{ij} + A_{ij} \exp(-b_{ij} r_{ij}) - c_{ij} / r_{ij}^6 \tag{1}$$

Here Φ_{ij} is the pairwise interaction energy between atoms i and j, and A_{ij}, b_{ij}, and c_{ij} are parameters which depend on the atomic species of atoms i and j. These parameters are reproduced in Table II. Charges q_i are also assigned, with $q_i = -1.2$ for O and 2.4 for Si. This Coulombic term was resummed using the Ewald method. The other two terms were summed out to a cutoff of 9.0 Å. The predictions of the model are only changed slightly by the introduction of this cutoff, as compared to the infinite–cutoff limit of the model.

For unstrained α–quartz, this implementation of the van Beest[2] model gives lattice constants $a = 4.92$ Åand $c = 5.44$ Å. The experimental values are $a = 4.9160$ and $c = 5.4054$[21]. To grow epitaxially on Si (100) (5.43 Å lattice constant) we set $a = c = 5.43$ Å in the surface plane, which gave a relaxed lattice constant normal to the surface of 8.60 Å. This amount of strain increased the energy of the quartz by 0.125 eV per SiO_2 molecule.

For cristobalite, we chose to multiply all distances (including our 9.0 Å radial cutoff) in the van Beest model by the factor 1.0227 to give better equilibrium properties. In particular, the rescaling was chosen so that the a axis would match experiment. The model then yields $a = 5.04$ Å and $c = 6.94$ Å, in good accord with experiment ($a = 5.042$ Å, $c = 7.131$ Å[22]). Cristobalite is tetragonal, so that the square base of 5.042 Å is stretched to epitaxially match the square Si lattice with period 5.43 Å. We found a relaxed value $c = 7.18$ Å normal to the surface. The strain energy in the cristobalite phase was found to be only 0.082 eV per

molecule.

For tridymite, all distances were rescaled by the same amount as for β–cristobalite. We found equilibrium lattice constants of $a = 5.00$ Å and $c = 8.30$ Å, again in good accord with experiment ($a = 5.03$ Å and $c = 8.22$ Å[23].) To observe the epitaxial strain, we set $a = 4.43$ Å and $c = 7.68$ Å in the surface plane, in order to match c and $\sqrt{3}a$ to $\sqrt{2}$ times the silicon lattice constant. The relaxed lattice constant normal to the surface was 5.42 Å. The strain energy for tridymite was 0.460 eV per molecule, a much higher value than for α–quartz or β–cristobalite.

For keatite, we multiplied all distances in the van Beest model by the factor 0.9811. As for other polymorphs, this constant was chosen to make the lattice constant along the surface directions match experiment. This gave equilibrium lattice constants $a = 7.456$ Å, and $c = 7.848$ Å, compared with experiment ($a = 7.456$, $c = 8.604$ Å[23]). The c axis is not in good accord with experiment, and is a shortcoming of the empirical potential. Epitaxial strain was introduced, setting $a = 7.678$ Å, in order to match the a axis with $\sqrt{2}$ times the silicon lattice constant. The relaxed lattice constant normal to the surface was 7.475 Å, and the strain energy was only 0.049 eV/molecule, and is the lowest strain energy for any of the polymorphs.

Epitaxial growth of the lowest strain energy structures, α–quartz, cristobalite, or keatite, seems plausible on the basis of energetics: we predict strain energies of 0.125 eV per molecule, 0.082 eV per molecule, and 0.049 eV per molecule for epitaxially grown structures (see Table I and Fig. 5). These values are comparable to the energy of the clathrasil structure melanophlogite, relative to α–quartz (0.1 eV per molecule[5]). Melanophlogite is an experimentally observed quartz polymorph.

Relative to the equilibrium van Beest *et al.* lattice constants of the unstrained material, α–quartz is expanded by 10.3% in one surface direction, and compressed by 0.2% in the other surface direction; cristobalite is expanded by 8.6% in both surface directions. Tridymite is compressed by 11.4% and 7.5% in the two surface directions. Since these strains are comparable, what accounts for the much greater strain energy of epitaxial tridymite? A

related finding is that the bulk moduli of the three phases are very different; values are B = 39.0 GPa for α–quartz, B = 18.8 GPa for β–cristobalite, and B = 138.3 GPa for tridymite[24], computed using the classical model of Tsuneyuki *et al.*[3]. Although the epitaxial strain is anisotropic, it is clear that tridymite is likely a "stiffer" structure than either α–quartz or β–cristobalite.

The very low strain energy of keatite probably stems from the relatively small (3.0%) expansion along the surface directions. The more complicated unit cell of this structure may make it a less attractive candidate for epitaxy, however, since it would require a more complicated concerted rearrangement of the atoms during oxidation. Also, despite the low strain energy we suspect the keatite structure itself may be significantly less stable than other silica polymorphs.

Fig. 6 is a histogram of the bond lengths for each silica phase with and without epitaxial strain. In the expanded structures of keatite, α–quartz, and β–cristobalite, the strain has the effect of enlongating bond lengths. Tridymite is compressed for epitaxy, and has correspondingly reduced bond lengths. The tetragonal symmetry of keatite and β–cristobalite is not broken by the epitaxial strain, hence the distribution of bond distances does not acquire more peaks, as is the case for α–quartz and tridymite.

Fig. 7 is a plot of the Si–O–Si bond angles for each silica phase. As for bond lengths, there is a trend toward larger angles in the structures which are expanded for epitaxy, and a trend toward smaller angles in tridymite, which is compressed for epitaxy. Fig. 8 is a plot of the O–Si–O bond angles for each silica phase. These angles are all reasonably close to the tetrahedral angle, 109.5 degrees; for the strained structures they range from 103 degrees to 123 degrees.

Besides the strain energy, there is the question of the total energy of one phase relative to another. Our calculations using the van Beest *et al.* model found unstrained α–quartz to be the most stable of the quartz, cristobalite, and tridymite set. Unstrained Cristobalite was 0.178 eV per molecule less stable than unstrained α–quartz, and unstrained tridymite was 0.255 eV per molecule less stable than unstrained α–quartz. Keatite was 0.153 eV per

molecule more stable than α–quartz, and coesite was 2.12 eV per molecule more stable than α–quartz. Given that α–quartz is the experimental ground state structure, it is clear that the relative stability of various crystal phases is poorly described by the van Beest *et al.* model, although the phases are dynamically stable, and their elastic properties are described well. Coesite has also been reported to be more stable than α–quartz for the classical empirical potential of Tsuneyuki et al.[3] which is a predecessor of the van Beest et al. model.

Tridymite requires a far larger strain energy of 0.460 eV per molecule to be epitaxial. This value is large enough that we think tridymite could not be formed epitaxially without mitigating circumstances. These might include strain relief by oxygen vacancies (as discussed by Chu and Fowler[25] in another context), dislocations, surface steps, or other types of disorder. Because tridymite can be deposited in two different orientations on the (100) silicon surface (see Ref.[10]), a certain amount of disorder is certainly inevitable.

The substantial strain energies required for epitaxy, at least for the polymorphs we considered, make it likely that crystalline to amorphous transition is driven by energetic considerations. The greater entropy of the amorphous state should also be a factor; at T= 1000 K, if there were one choice of bonding orientation per molecule, this would give a free energy contribution of $kTlog(2) = 0.06$ eV per molecule. These considerations may allow various defects to coalesce in existing silica, as new growth occurs at the interface.

Because silica has pronounced ionic character, we believe atomic charges are important in generating surface reconstructions (see Ref.[26]) and interfacial order. Furthermore, atomic charges seem necessary to generate correct elastic properties–although the local environment is very similar in cristobalite and tridymite, bulk moduli differ by a factor of seven, and the structures substantially differ in stability. The long–range character of atomic interactions seemingly ensures that interfacial charge and dipole layers will affect oxidation. We plan to consider these phenomena more carefully in future work.

ACKNOWLEDGMENTS

We thank the National Science Foundation (DMR 95-26274) for support of this work. We would also like to thank Nicole Herbots for many helpful comments.

This work is performed under the auspices of U.S. Department of Energy and Lawrence Livermore National Laboratory under contract No. W-7405-Eng-48.

REFERENCES

[1] An attempt was made to consider coesite, but we could find no easy way to generate an epitaxial interface given the staggered bonding of this structure, and the potential model we are using in this work is inadequate for coesite.

[2] B. W. H. van Beest, G. J. Kramer, and R. A. van Santen, Phys. Rev. Lett. **64** 1955 (1990); G. J. Kramer, N. P. Farragher, B. W. H. van Beest, and R. A. van Santen, Phys. Rev. B **43** 5068 (1991).

[3] S. Tsuneyuki, M. Tsukada, H. Aoki, and Y. Matsui, Phys. Rev. Lett. **61** 869 (1988); S. Tsuneyuki, Y. Matsui, H. Aoki, and M. Tsukada, Nature **339** 209 (1989).

[4] J. R. Chelikowsky, H. E. King, Jr., J. Glinnemann, Phys. Rev. B **41** 10866 (1990).

[5] A. A. Demkov, J. Ortega, O. F. Sankey, and M. P. Grumbach, Phys. Rev. B **52** 1618 (1995).

[6] Y. Iida, T. Shimura, J. Harada, S. Samata, and Y. Matsushita, Surf. Sci. **258** 235 (1991).

[7] I. Takahashi, T. Shimura, and J. Harada, J. Phys. Condens. Matter **5** 6525 (1993).

[8] I. Takahashi, K. Nakano, J. Harada, T. Shimura, and M. Umeno, Surf. Sci. **315**, L 1021 (1994).

[9] P. H. Fuoss, L. J. Norton, S. Brennan, and A. Fischer–Colbrie, Phys. Rev. Lett. **60** 600 (1988).

[10] A. Ourmazd, D. W. Taylor, J. A. Rentschler, and J. Bevk, Phys. Rev. Lett. **59** 213 (1987); A. Ourmazd, P. H. Fuoss, J. Bevk, and J. F. Morar, Appl. Surf. Sci. **41/42**, 365 (1989).

[11] G. Y. Fan, J. M. Cowley, and J. C. H. Spence, Phys. Rev. Lett. **58** 282 (1987).

[12] A. Ourmazd, J. C. Bean, and J. C. Phillips, Phys. Rev. Lett. **58** 283 (1987).

[13] To be submitted, N. Herbots et al.

[14] A. A. Demkov *et al.* in preparation, and Bull. Am. Phys. Soc. **43** 621 (1998).

[15] A. Pasquarello, M. S. Hybertsen, and R. Car, unpublished, Bull. Am. Phys. Soc. **43** 446 (1998).

[16] T. Hattori, T. Igarashi, M. Ohi, and H. Yamagishi, Jpn. J. Appl. Phys. **28** L 1436 (1989).

[17] F. Herman and R. V. Kasowski, J. Vac. Sci. Technol. **19** 395 (1981).

[18] M. Hane, Y. Miyamoto, and A. Oshiyama, Phys. Rev. B **41** 12637 (1990).

[19] H. Kageshima and K. Shiraishi, Surface Science **380** 61 (1995).

[20] A. Pasquarello, M. S. Hybertsen, and R. Car, Appl. Phys. Lett. **68** 625 (1996); Phys. Rev. Lett. **74** 1024 (1995); Phys. Rev. B **53** 10942 (1996).

[21] L. Levien, C. T. Prewitt, and D. J. Weidner, Am. Mineral. **65** 920 (1980).

[22] A. F. Wright and A. J. Leadbetter, Philos. Mag. **31**, 1391 (1975).

[23] R. W. G. Wyckoff, *Crystal Structures*, 4th ed. (Interscience, New York, 1974), and the references therein.

[24] N. R. Keskar and J. R. Chelikowsky, Phys. Rev. B **46** 1 (1992).

[25] A. X. Chu and W. B. Fowler, Phys. Rev. B **41**, 5061 (1990).

[26] W. A. Harrison, J. Vac. Sci. Technol. **16** 1492 (1979).

FIGURES

FIG. 1. An interface between silicon (lower atoms) and β–cristobalite (upper atoms). View rotated 90 degrees is identical. The vertical direction is the Si (100) axis and the direction into the page is Si (010). The oxygen atoms are the small solid circles in the upper half of the figure.

FIG. 2. An interface between silicon (lower atoms) and tridymite (upper atoms), from two perspectives. In (a), the vertical direction is the Si (100) axis and the direction into the page is Si (110). In (b), the structure is rotated 90 degrees so that Si (110) lies in the plane of the page. The oxygen atoms are the small solid circles in the upper half of each figure.

FIG. 3. An interface between silicon (lower atoms) and α–quartz (upper atoms), from two perspectives. In (a), the vertical direction is the Si (100) axis and the direction into the page is Si (100). In (b), the structure is rotated 90 degrees so that Si (100) lies in the plane of the page. The oxygen atoms are the small solid circles in the upper half of each figure.

FIG. 4. An interface between silicon and keatite, from two perspectives. In (a), the vertical direction is the Si (100) axis and the direction into the page is Si (110). In (b), the structure is rotated 90 degrees so that Si (100) lies in the plane of the page. The oxygen atoms are the small solid circles in the upper half of each figure.

FIG. 5. Strain energy of thin layers of four silica polymorphs as a function of layer thickness. The intercept of these energy curves has been chosen to be zero so that only the slope is meaningful. Also the relative energies of the silica polymorphs is not taken into account; only the strain energy is indicated.

FIG. 6. Bond length histograms for four silica polymorphs at equilbrium with epitaxial strain (solid bars) and without epitaxial strain (gray bars).

FIG. 7. Plot of Si–O–Si angles for four silica polymorphs at equilibrium with epitaxial strain (black line) and without epitaxial strain (gray line).

FIG. 8. Plot of O–Si–O angles for four silica polymorphs at equilibrium with epitaxial strain (black line) and without epitaxial strain (gray line).

TABLES

TABLE I. The strain and total energies for the silica polymorph studies. Strains are given as percent, and parallel (||) and perpendicular ($\perp$) refer to direction relative to the Si (100) interface. E_0 is the energy of the perfect crystalline silicon polymorph at its minimum energy geometry, where α–quartz is defined as zero energy. E_{strain} is the energy above E_0 due to strain effects, due to the epitaxial strain. All energies are per SiO_2 molecule.

Structure	E_0 (eV)	$\epsilon_1^{\parallel}$	$\epsilon_2^{\parallel}$	$\epsilon_{\perp}$	E_{strain} (eV)	$E_0 + E_{strain}$
α–quartz	0	10.3	-0.2	0.9	0.125	0.125
β–cristobalite	0.178	8.6	8.6	3.4	0.082	0.260
tridymite	0.255	-11.4	-7.5	8.4	0.460	0.715
keatite	-0.153	3.0	3.0	-4.8	0.049	-0.104

TABLE II. Empirical potential parameters, for the model of van Beest et al.[2]

	Parameters			Atomic
i–j	A_{ij} (eV)	b_{ij} (Å^{-1})	c_{ij} (eV Å^6)	charges
O–O	1388.7730	2.76000	175.0000	$q_O = -1.2$
Si–O	18003.7572	4.87318	133.5381	$q_{Si} = 2.4$

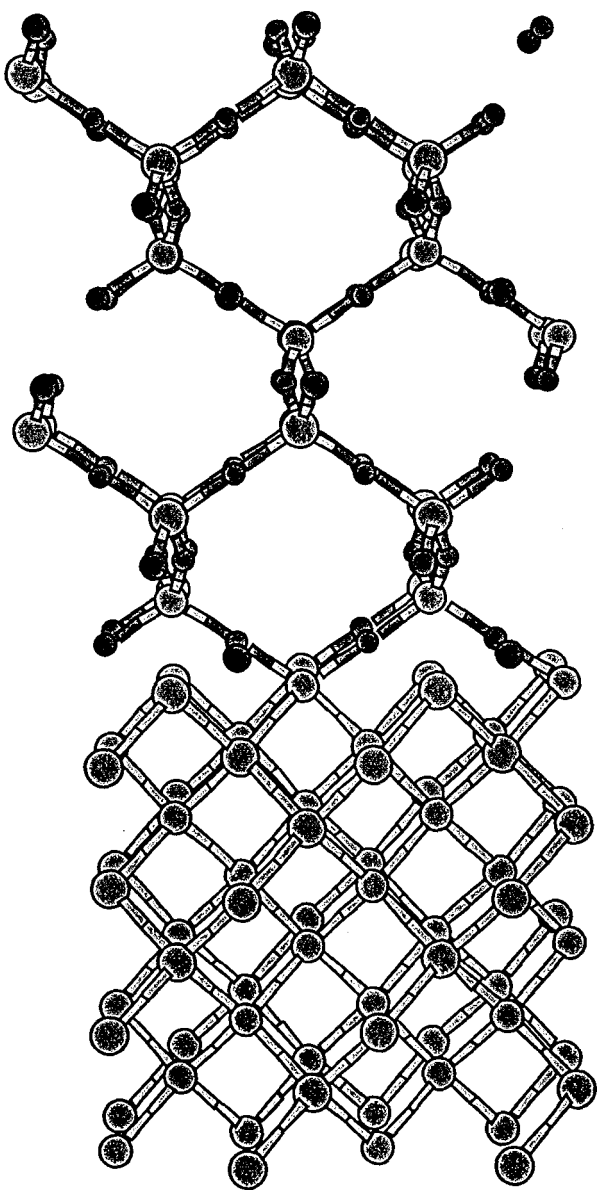

Fig 1

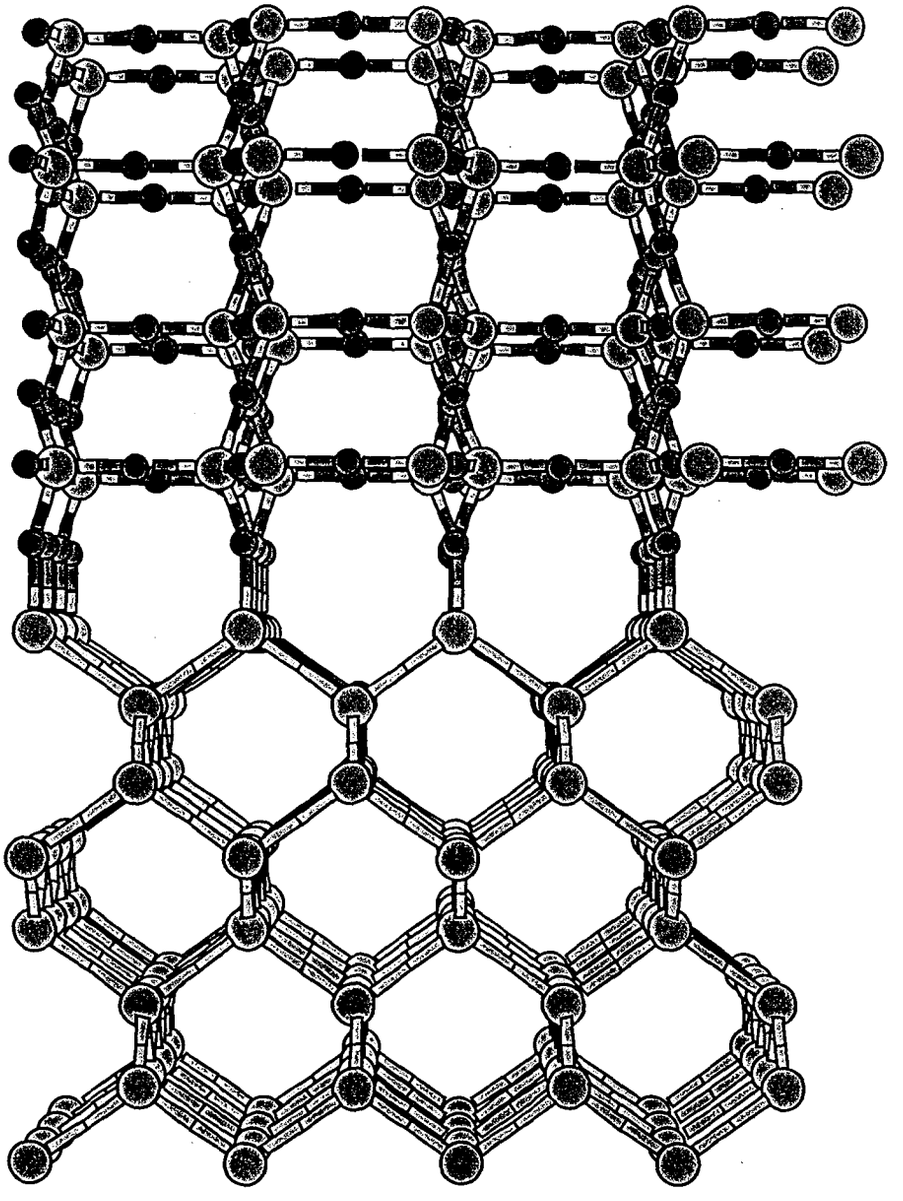

Fig 2a

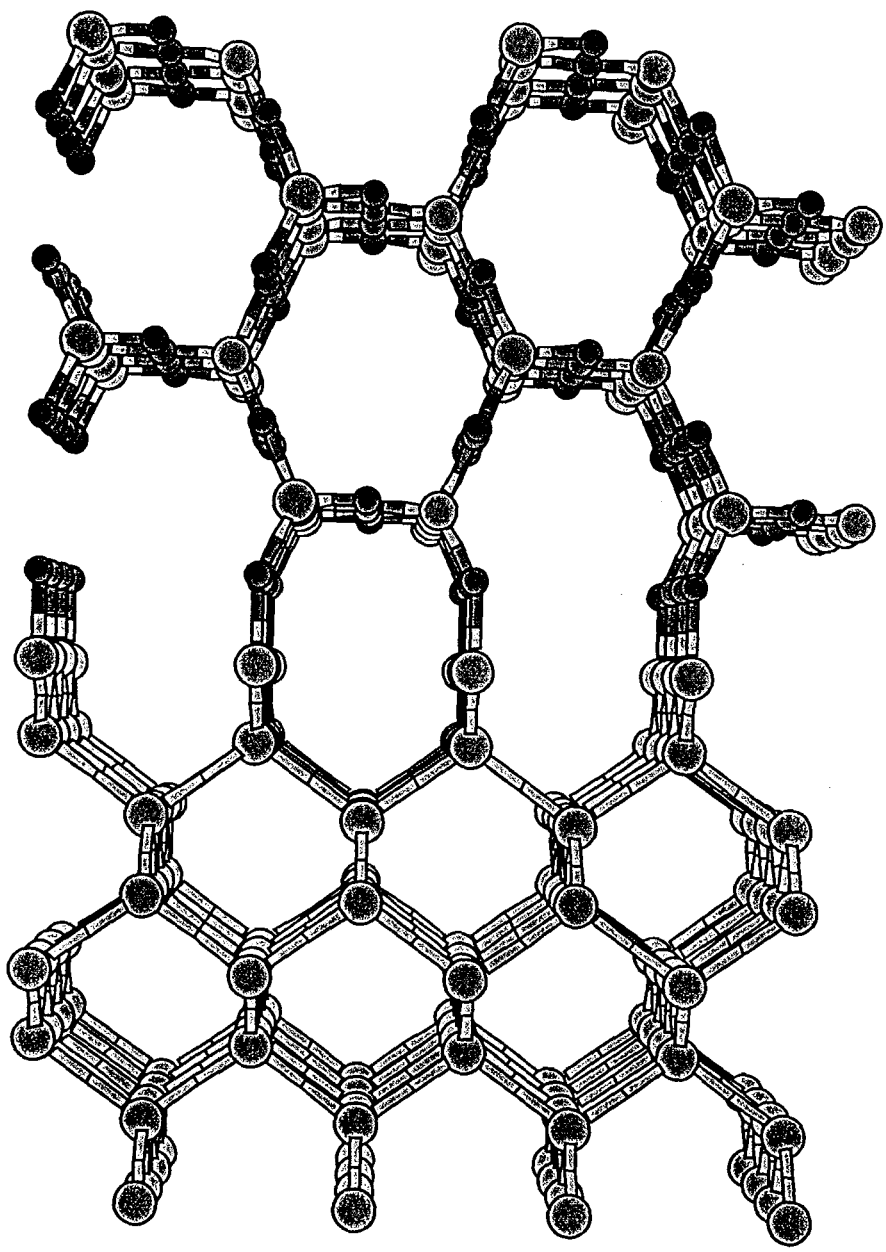

Fig 26

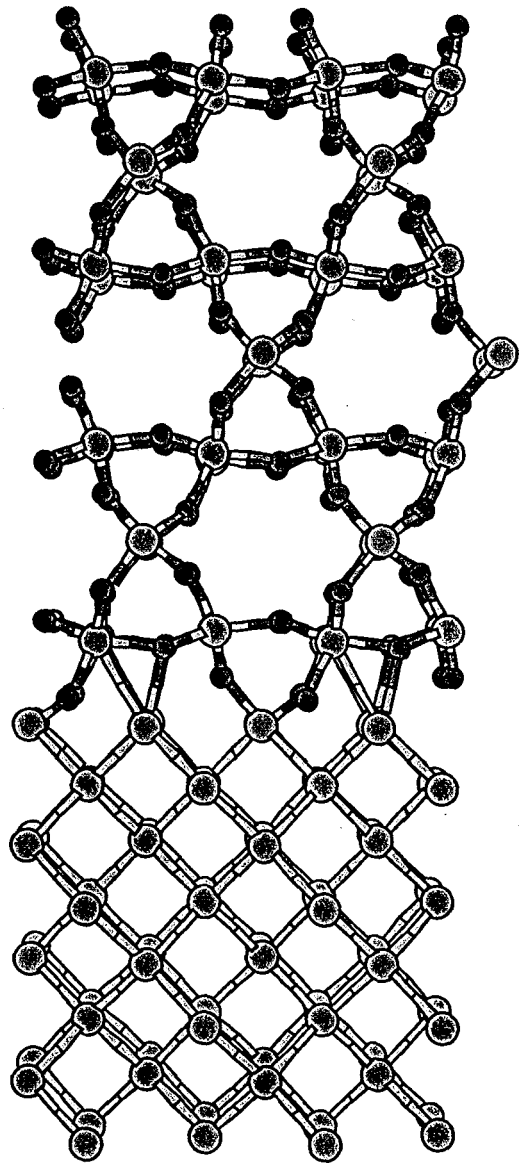

Fig 3a

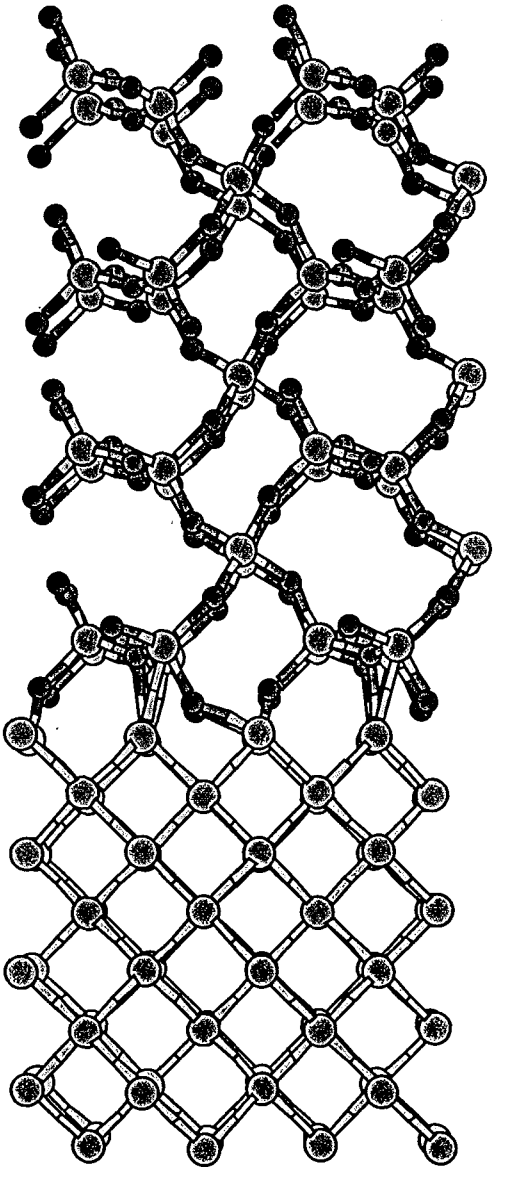

Fig 3b

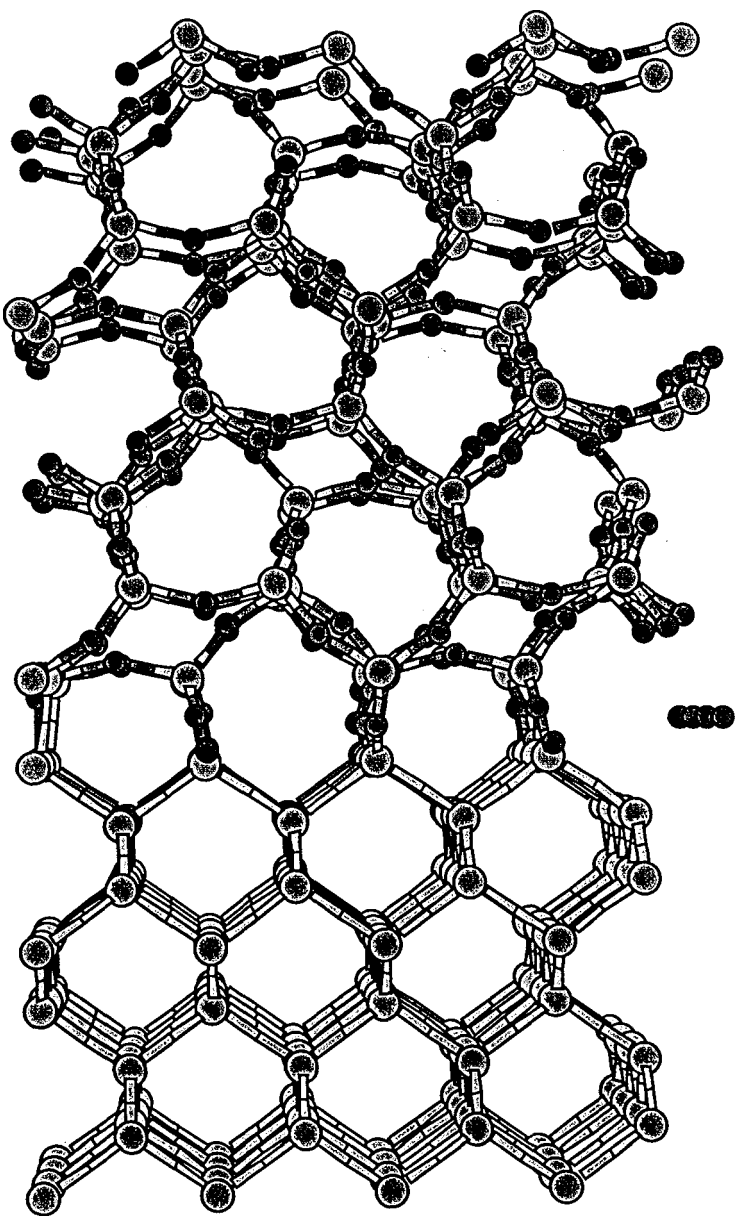

Fig 4a

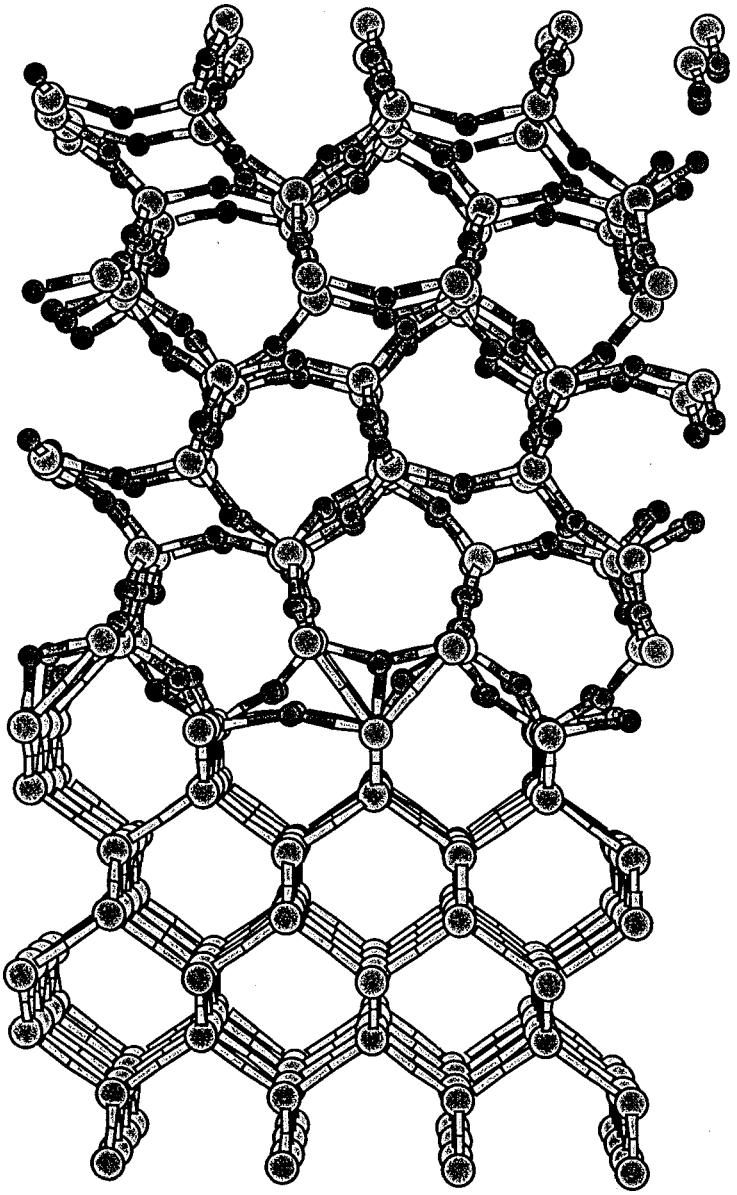

Fig 46.

Strain energy per unit area vs. Thickness

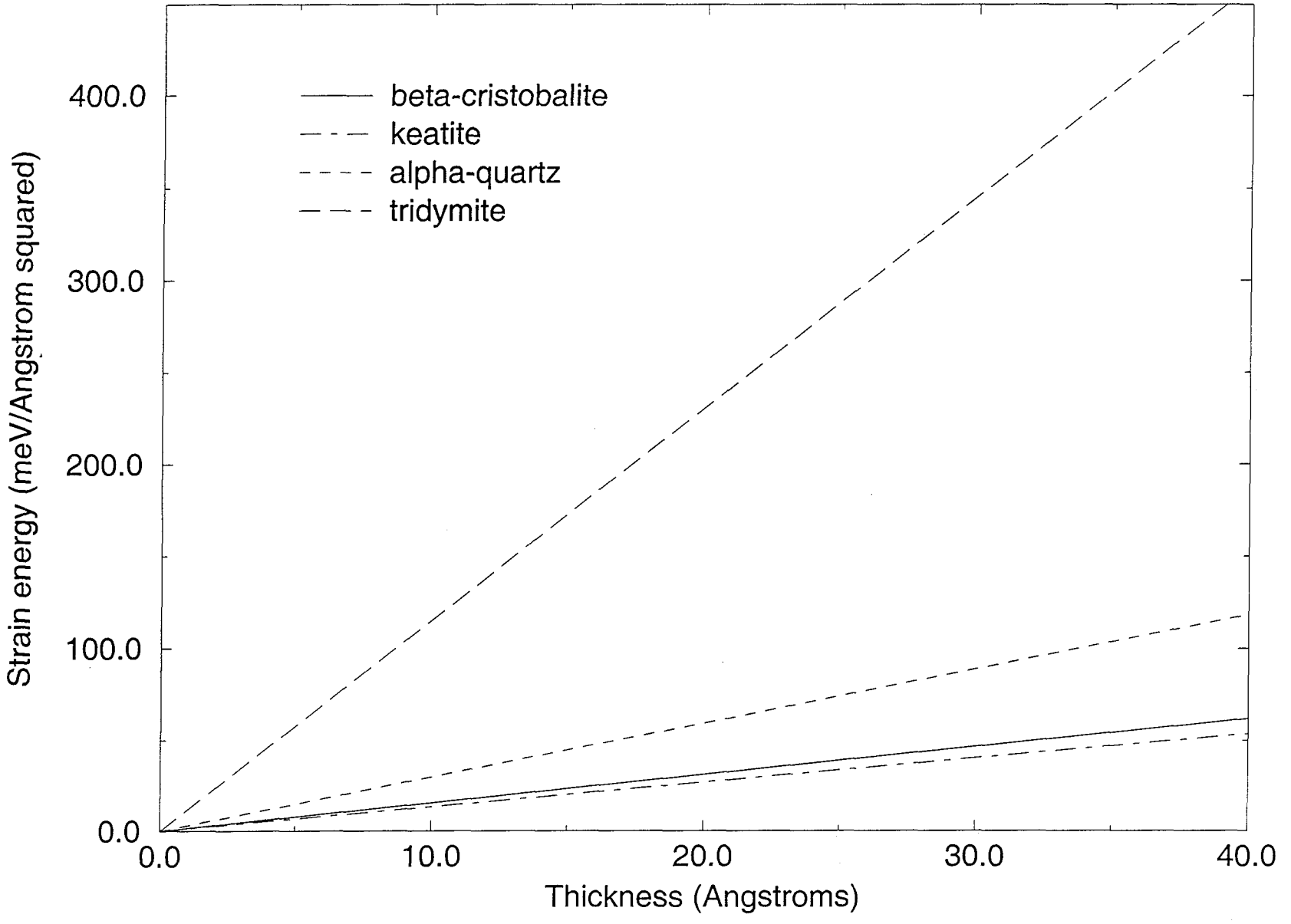

Fig 5

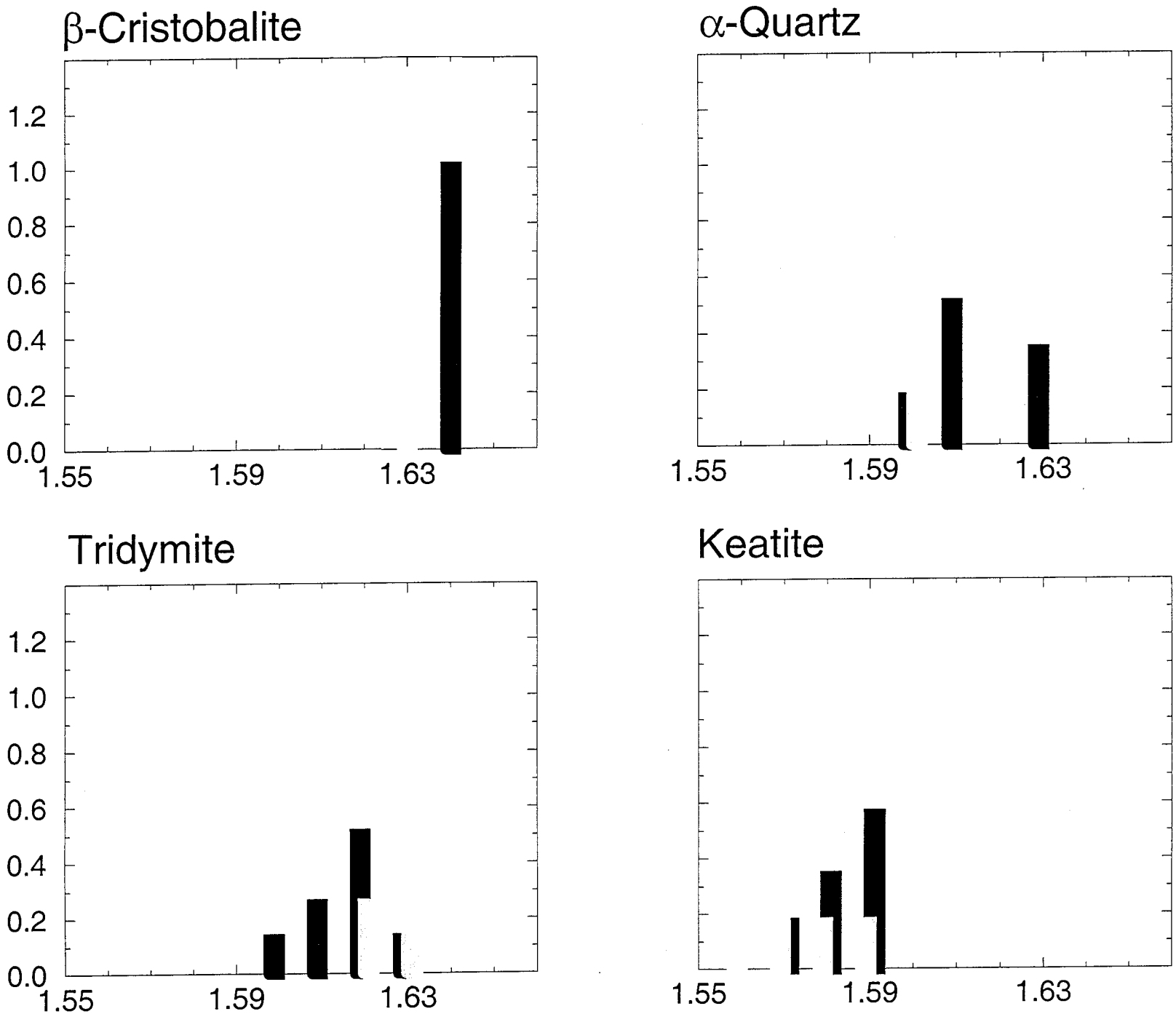
β-Cristobalite
α-Quartz
Tridymite
Keatite
1.2
1.0
0.8
0.6
0.4
0.2
0.0
1.55
1.59
1.63

Fig 6

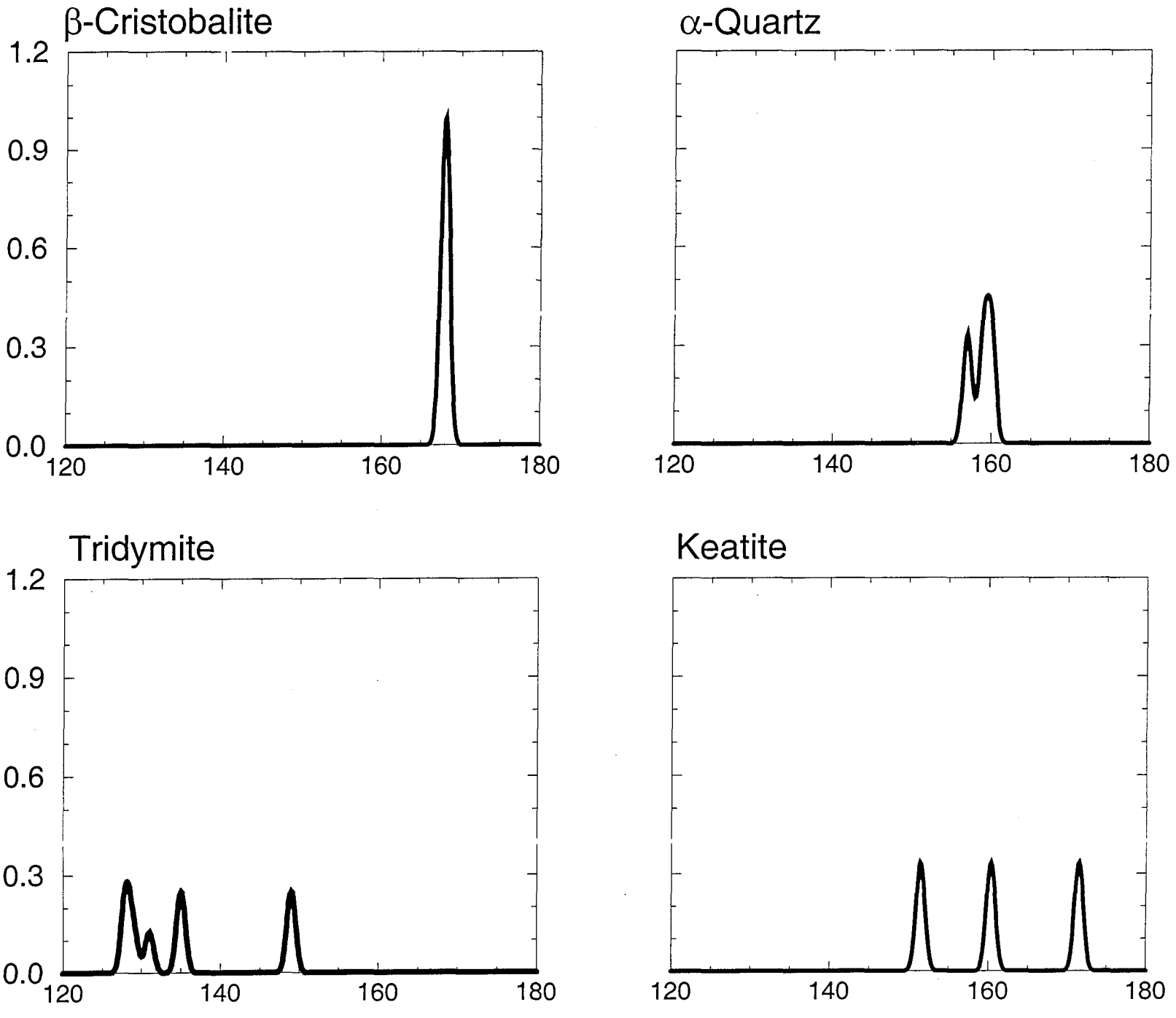
β-Cristobalite
α-Quartz
Tridymite
Keatite
1.2
0.9
0.6
0.3
0.0
120
140
160
180

Fig. 7

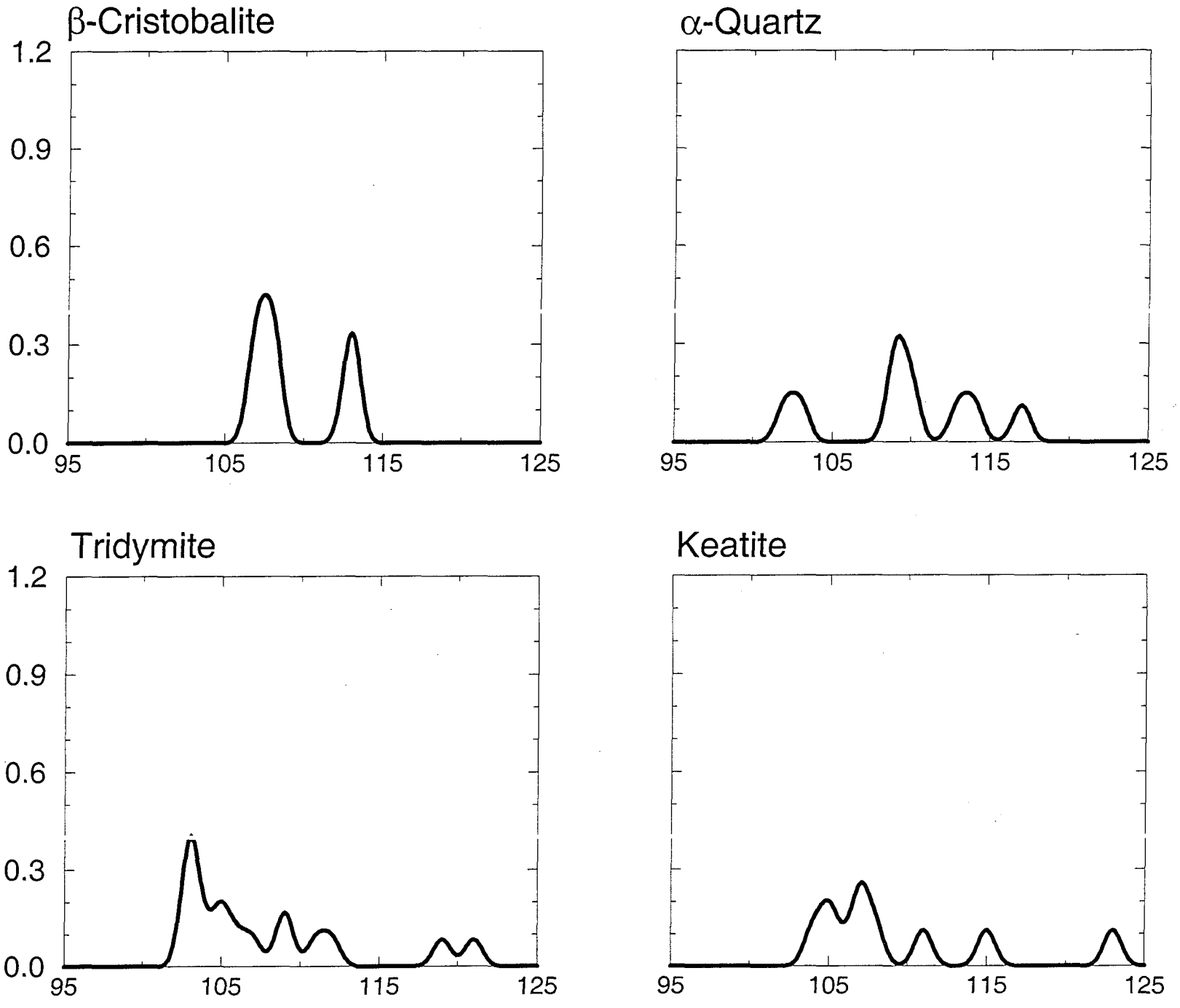
β-Cristobalite
α-Quartz
Tridymite
Keatite
1.2
0.9
0.6
0.3
0.0
95
105
115
125

Fig 8